

New Cooling Technology Magnetic Cooling and Magnetocaloric Properties of $\text{La}_{0.85}\text{Ag}_{0.15}\text{MnO}_3$ and $(\text{La}_{0.8}\text{Pr}_{0.2})_{0.85}\text{Ag}_{0.15}\text{MnO}_3$ Compounds

*¹Ali Osman Ayaş, ²Ahmet Ekicibil

¹Department of Physics, Faculty of Sciences and Letters, Adiyaman University, 02040 Adiyaman, Turkey

²Department of Physics, Faculty of Sciences and Letters, Çukurova University, 01330 Adana, Turkey

Abstract

In this work, firstly new, environmentally friendly and energy efficient technology called as magnetic cooling (MC) based on magnetocaloric effect (MCE) [1-5] and the materials which are produced as a candidate cooling materials has been introduced. Then the structural and magnetic properties of the polycrystalline $\text{La}_{0.85}\text{Ag}_{0.15}\text{MnO}_3$ (LAM) and $(\text{La}_{0.8}\text{Pr}_{0.2})_{0.85}\text{Ag}_{0.15}\text{MnO}_3$ (LPAM) compounds prepared by the sol-gel method, were investigated. The structural properties of the samples were studied by employing XRD, SEM and EDX measurements. The XRD results have shown that both of our synthesized samples have crystallized in the hexagonal symmetry with $R\bar{3}c$ space group. SEM and EDX observations show that the particles are closely packed, their size range from $0.5\mu\text{m}$ to $2.0\mu\text{m}$ with the average sizes of $1.23\mu\text{m}$ and $1.03\mu\text{m}$ for LAM and LPAM, respectively. The magnetic properties were studied by employing $M(T)$ and $M(H)$ measurements. Both compounds show magnetic phase transition from paramagnetic to ferromagnetic phase. With the substituting of Pr for La, the Curie temperature, T_C , decreases from 262 K to 216 K. At a field change of 1T LAM and LPAM show large magnetic entropy changes of 4.13 and 4.03 J/kgK, respectively. Furthermore their relative cooling power (RCP) values are 16.52 and 32.24 J/kg, respectively. Arrot plots reveal second order magnetic phase transition for both samples. These properties make both LAM and LPAM compounds good candidates for the practical magnetic refrigeration [2,6-8].

Key words: Environmentally Friendly Technology, Magnetocaloric effect, Magnetic entropy.

*Corresponding Author:

Dr. Ali Osman AYAŞ

Department of Physics,

Faculty of Sciences and Letters,

Adiyaman University, 02040 Adiyaman, Turkey

e-mail: aayas@adiyaman.edu.tr

1. Introduction

Magnetocaloric effect (MCE) provides a unique way of realizing the refrigeration from ultra-low to room temperatures. By increasing the magnetic field, magnetic entropies decrease and heat is radiated from the magnetic system into the environment through an isothermal process, on the contrary while by decreasing the magnetic field, magnetic entropies increase and heat is absorbed from the lattice system into the magnetic system through an adiabatic process.

Due to the promising environmentally friendly and energy efficient magnetic cooling systems comparing with the well-known gas-compression refrigeration, room temperature magnetic cooling based on MCE has attracted attention in recent years [1]. MCE has been studied in a large variety of magnetic materials [2]. Among these, perovskite manganites of the general formula $R_{1-x}A_xMnO_3$ (R: rare-earth cation, A: alkali-metal or alkaline-earth cation) have proven to be beneficial for potential applications because of their interesting properties such as convenient preparation, exhibiting high chemical stability, higher resistivity (which lowers eddy currents) and much smaller thermal and field hysteresis than any rare earth and 3d-transition metal based alloys, and cheapest material among existing magnetic refrigerants [3-10]. Furthermore, the Curie temperatures and saturation magnetizations of these materials can be adjusted by varying their compositions [5, 7-8]. Among manganites the $La_{1-x}Ag_xMnO_3$ ($0.0 \leq x \leq 1.0$) series are one of the most famous materials; for instance $T_C = 306K$ for $x = 0.3$ (near room temperature) and a large magnetic entropy change of $3.40J/kgK$ for $x = 0.2$ is observed under 1 T magnetic field change [11]. Additionally there are a lot of further works about $La_{1-x}Ag_xMnO_3$ series but in the literature there is no work about Pr-substitution to this series. So in this study we have selected Ag-based $La_{0.85}Ag_{0.15}MnO_3$ (LAM) and some Pr-substituted for La to obtain $(La_{0.8}Pr_{0.2})_{0.85}Ag_{0.15}MnO_3$ (LPAM) compound to explore the magnetocaloric properties of them and to find new magnetocaloric materials to evaluate their refrigeration efficiency with applicability at various temperature intervals. As a result in this work we report the magnetocaloric properties of LAM with and without the effect of doping $0.17Pr^{3+}$ to the A site.

2. Experimental Procedure

Polycrystalline powder samples of $La_{0.85}Ag_{0.15}MnO_3$ (LAM) and $(La_{0.8}Pr_{0.2})_{0.85}Ag_{0.15}MnO_3$ (LPAM) were prepared by the so called sol-gel method by using high purity powders of La_2O_3 , $Mn(NO_3)_2 \cdot 4H_2O$ and $AgNO_3$ for LAM and La_2O_3 , $Pr(NO_3)_3 \cdot 6H_2O$, $Mn(NO_3)_2 \cdot 4H_2O$ and $AgNO_3$ for LPAM as starting materials. The final materials were grounded by using an agate mortar to obtain fine powder. After that, the microcrystalline powder was pressed into disks and sintered at $970^\circ C$ for 24 h in air. The crystal structure of the powder sample was determined by X-ray diffraction (XRD) using $Cu K\alpha$ radiation, the grain structure was observed with a scanning electron microscope (SEM), morphological and compositional properties investigated by energy-dispersive X-ray

spectroscopy (EDX). The temperature dependence and the magnetic field dependences of the magnetization, $M(T)$ and $M(H)$, were measured using a Vibration Sample Magnetometer. The magnetic entropy change ΔS_M was obtained from isothermal magnetization curves.

3. Results and Discussions

On the basis of crystallographic data, the unit cell parameters computed and are given in Table 1. It is clear from the Table 1 that unit cell volume and parameters decrease with the substitution of Pr for La. This decrease can be linked to the replacement of Pr^{3+} with La^{3+} which leads to decrease A site average ionic radius due to the smaller ionic radius of Pr^{3+} compared to that of La^{3+} [12, 14].

In order to obtain a better insight on the microstructure of the compounds, SEM and EDX investigations were also carried out. The SEM images of samples revealed that the samples are constituted of closely packed homogeneous particles, ranging from $0.5\mu\text{m}$ to $2.0\mu\text{m}$; average particle size calculated from SEM images are $1.23\mu\text{m}$ and $1.03\mu\text{m}$ for LAM and LPAM, respectively. From the exchange of some La peak in the LAM with the Pr peaks in the LPAM and the similarity of these peak intensities and trace lines, it can be concluded that Pr was successfully integrated into the crystal structure of LAM. All the locations in the bulk materials contained the expected elements (La, Pr, Ag and Mn) which confirms that there is no loss of any integrated elements during the sintering and there is no other impurity elements.

The transition temperatures, T_C , obtained from the minimum of the derivatives of $M(T)$ curve's dM/dT are listed in Table 2, along with that of the other Ag based manganites. According to the Table 2, T_C decreases from 262 K to 216 K by the substitution of Pr for La in LAM. This decrease in T_C can be explained in terms of decreasing the average A-site cation size $\langle r_A \rangle$ [12, 14]. It is believed that ferromagnetism in undoped $\text{La}_{0.85}\text{Ag}_{0.15}\text{MnO}_3$ sample is linked to ferromagnetic Mn^{3+} - Mn^{4+} Double Exchange (DE) interaction leading to a maximum magnetic transition temperature of 262 K with the optimum $\text{Mn}^{4+}/(\text{Mn}^{3+} + \text{Mn}^{4+})$ ratio of 0.30. It should be noted that Pr^{3+} addition to LAM cannot influence the $\text{Mn}^{4+}/(\text{Mn}^{3+} + \text{Mn}^{4+})$ ratio. If the oxidation state of Pr ions entering to the structure is taken to be a mixture of 2+ and 3+, then the ionic balance of compound can be written as $(\text{La}_{0.8}^{3+}\text{Pr}_{0.2-x}^{3+}\text{Pr}_x^{2+})_{0.85}\text{Ag}_{0.15}^{1+}\text{Mn}_{0.7-0.85x}^{3+}\text{Mn}_{0.3+0.85x}^{4+}\text{O}_3$ where the x is the content of Pr^{2+} in

the compound. So the content of Mn^{4+} in the structure can vary in between 0.3 and 0.5. This probability may also be the reason of reducing the T_C , because the optimum $Mn^{4+}/(Mn^{3+}+Mn^{4+})$ ratio changes by joining of Pr^{2+} into the structure leading to a weakened DE interaction hence an AFM interaction may be favoured [13-15].

Fig. 1.a-b show the isothermal magnetization curves for $La_{0.85}Ag_{0.15}MnO_3$ (from 240 K to 286 K) and $(La_{0.8}Pr_{0.2})_{0.85}Ag_{0.15}MnO_3$ (from 196 K to 240 K) samples. These M-H curves were obtained at temperature intervals of 4 K both below and above the Curie temperatures of the samples with respect to the external applied magnetic fields in between 0 and 1 T. Based on the thermodynamic theory, the magnetic entropy change, (ΔS_M), which results from the spin ordering and which is induced by the variation of the applied magnetic field from 0 to H_{max} , can be derived from the thermodynamic Maxwell relation [16],

$$\left(\frac{\partial S}{\partial H}\right)_T = \left(\frac{\partial M}{\partial T}\right)_H \quad (1)$$

through integrating over the magnetic field H,

$$\Delta S_M(T, H) = \int_0^{H_{max}} \left(\frac{\partial M}{\partial T}\right) dH \quad (2)$$

where H_{max} is the final applied magnetic field. According to the Eq. (2), the magnetic entropy change ΔS_M depends on the temperature gradient of the magnetization and attains a maximum value around Curie temperature, at which the magnetization decays most rapidly. For magnetization measured at discrete field and temperature intervals, the magnitude of the magnetic entropy change defined in Eq. (2) can be approximated by Eq. (3) [17],

$$|\Delta S_M(T, H)| = \sum_i \frac{M_i - M_{i+1}}{T_{i+1} - T_i} \Delta H \quad (3)$$

where M_i and M_{i+1} are magnetization values measured at temperatures T_i and T_{i+1} , respectively. The entropy changes, $\Delta S_M(T)$, versus temperature at 0.5 and 1 T applied magnetic fields for both samples are shown in Fig. 2.a-b. The maximum of the magnetic entropy change observed for LAM and LPAM is found to be 4.13 and 4.03 J/kgK at 1 T applied magnetic field, respectively. These values are larger than that of Gd [18] and most of the reported

perovskite materials (see also Table 2) and hence these results are high enough to make our samples potential candidates for magnetic refrigeration.

From the cooling perspective, it is important to consider not only the magnitude of the magnetic entropy change but also the refrigerant capacity (RC), which correspond to the amount of heat transferred between the cold and the hot sinks in the ideal refrigeration cycle defined by

$$\text{RCP} = |\Delta S_M| \times \delta T_{\text{FWHM}}, \quad (4)$$

where δT_{FWHM} is the full width at half-maximum of the ΔS_M curve [19]. For our samples the RCP values at $\Delta H = 1\text{T}$ are 16.52 and 32.24 J/kg for LAM and LPAM, respectively. As a result we should indicate that the RCP values increase while ΔS_M values decrease by substitution of Pr for La. RCP value of LPAM is comparable with the reported values [2].

To determine the nature of the magnetic transition of the samples, Arrot plots of H/M versus M^2 covering a broad temperature range around T_C are plotted in Fig. 3a-b. Positive slopes are clearly observed from Fig. 3a-b, indicating the occurrence of the second order magnetic phase transition.

4. Conclusions

We have investigated the structural, magnetic and magnetocaloric properties of polycrystalline $\text{La}_{0.85}\text{Ag}_{0.15}\text{MnO}_3$ and Pr-substituted $(\text{La}_{0.8}\text{Pr}_{0.2})_{0.85}\text{Ag}_{0.15}\text{MnO}_3$ samples produced by the sol-gel method. XRD results show that our both sample are crystallize in the rhombohedral structure with $R\bar{3}c$ space group (hexagonal setting). Unit cell volume and parameters decrease with the substitution of Pr for La. SEM observation shows that the particles are closely packed and their sizes range from $0.5\mu\text{m}$ to $2.0\mu\text{m}$ with the average particle size of $1.23\mu\text{m}$ and $1.03\mu\text{m}$ for LAM and LPAM respectively. From the EDX data it can be concluded that Pr was successfully integrated into the crystal structure of LAM and there is no loss of any integrated elements during the sintering and there is no other impurity elements. The ferromagnetic to paramagnetic phase transitions observed at $T_C \sim 262$ and 216K for LAM and LPAM, respectively; T_C reduces via Pr-substitution for La and the Arrot plots reveal the second order nature of magnetic transitions for both samples. We have found large magnetic entropy changes, large magnetocaloric effect, for both samples. They are about 4.13 and

4.03J/kgK at 1T applied magnetic field change. Furthermore, the RCP values at a field change of $\Delta H = 1 \text{ T}$ are 16.5 and 32.2 J/kg for LAM and LPAM, and are comparable with that of the familiar/well-known magnetic refrigerant materials. All these results indicate that the LAM and LPAM could be considered as good candidates for magnetic refrigeration.

Acknowledgements

This work is supported by the Research Fund of Çukurova University, Adana, Turkey, under grant contracts no. FEF2013BAP16 and no. FEF2010D11.

References

- [1] V.K. Pecharsky, K.A. Gschneidner Jr., J. Appl. Phys. 86 (1999) 565.
- [2] M.H. Phan, S.C. Yu, J. Magn. Magn. Mater. 308 (2007) 325–340.
- [3] Z. Wang, Q. Xu, G. Ni, H. Zhang, Physica B 406 (2011) 4333–4337.
- [4] V.S. Kolat, T. Izgi, A.O. Kaya, N. Bayri, H. Gencer, S. Atalay, J. Magn. Magn. Mater. 322 (2010) 427–433.
- [5] M.H. Phan, S.B. Tian, D.Q. Hoang, S.C. Yu, C. Nguyen, A.N. Ulyanov, J. Magn. Magn. Mater. 25–259 (2003) 309–311.
- [6] N. Chau, H.N. Nhat, N.H. Luong, D.L. Minh, N.D. Tho, N.N. Chau, Physica B 327 (2003) 270–278.
- [7] J. Fan, L. Pi, L. Zhang, W. Tong, L. Ling, B. Hong, Y. Shi, W. Zhang, D. Lu, Y. Zhang, Physica B 406 (2011) 2289–2292.
- [8] S. K. Çetin, M. Acet, A. Ekicibil, C. Sarıkürkçü, K. Kıymaç, Journal of Alloys and Compounds 565 (2013) 139–143
- [9] M.H. Phan, S.C. Yu, J. Magn. Magn. Mater. 308 (2007) 325–340.
- [10] A. Rebello, V.B. Naik, R. Mahendiran, J. Appl. Phys. 110 (2011) 013906.
- [11] T. Tang, K.M. Gu, Q.Q. Cao, D.H. Wang, S.Y. Wang, S.Y. Zhang, Y.W. Du, J. Magn. Magn. Mater. 222 (2000) 110.
- [12] T.D. Thanh, L.H. Nguyen, D.H. Manh, N.V. Chien, P. T. Phong, N. V. Khiem, L. V. Hong, N. X. Phuc, Physica B 407 (2012) 145–152
- [13] A. Dhahri, J. Dhahri, E. Dhahri, Journal of Alloys and Compounds 489 (2010) 9–12
- [14] N. Kallel, S. Kallel, A. Hagaza, M. Oumezzine, Physica B 404 (2009) 285–288.
- [15] Y. Samancıoğlu, A. Coşkun, Journal of Alloys and Compounds 507, (2010) 380–385
- [16] A.H. Morrish, The Physical Principles of Magnetism, Wiley, New York, 1965 (Chapt.3).
- [17] M. Foldeaki, R. Chahine, T.K. Bose, J. Appl. Phys. 77 (1995) 3528.
- [18] J.S. Lee, Phys. Status Solidi (b) 241 (2004) 1765.
- [19] K.A. Gschneidner, V.K. Pecharsky, Annu. Rev. Mater. Sci. 30 (2000) 387.

Table 1. Cell parameters of $\text{La}_{0.85}\text{Ag}_{0.15}\text{MnO}_3$ and $(\text{La}_{0.8}\text{Pr}_{0.2})_{0.85}\text{Ag}_{0.15}\text{MnO}_3$ samples from X-ray diffraction measurements.

Sample Codes	a (Å)	b (Å)	c (Å)	V (Å ³)
LAM	5.522	5.522	13.373	353.24
LPAM	5.511	5.511	13.298	349.81

Table 2. The maximum magnetic entropy changes and the corresponding Curie temperature for Ag based samples.

Sample	T _C (K)	-ΔS _M (J/kgK)	μ _{eff}	ΔH (T)	Reference
La _{0.95} Ag _{0.05} MnO ₃	214	1.10	N.A.	1	12
La _{0.80} Ag _{0.20} MnO ₃	278	3.40	N.A.	1	12
La _{0.80} Ag _{0.20} MnO ₃	300	2.40	N.A.	1	13
La _{0.78} Ag _{0.22} MnO ₃	306	2.90	N.A.	1	13
La _{0.75} Ag _{0.25} MnO ₃	306	1.52	N.A.	1	12
La _{0.70} Ag _{0.30} MnO ₃	306	1.35	N.A.	1	12
La _{0.85} Ag _{0.15} MnO ₃	262	4.13	4.17	1	Present work
(La _{0.80} Pr _{0.2}) _{0.85} Ag _{0.15} MnO ₃	216	4.03	4.07	1	Present work

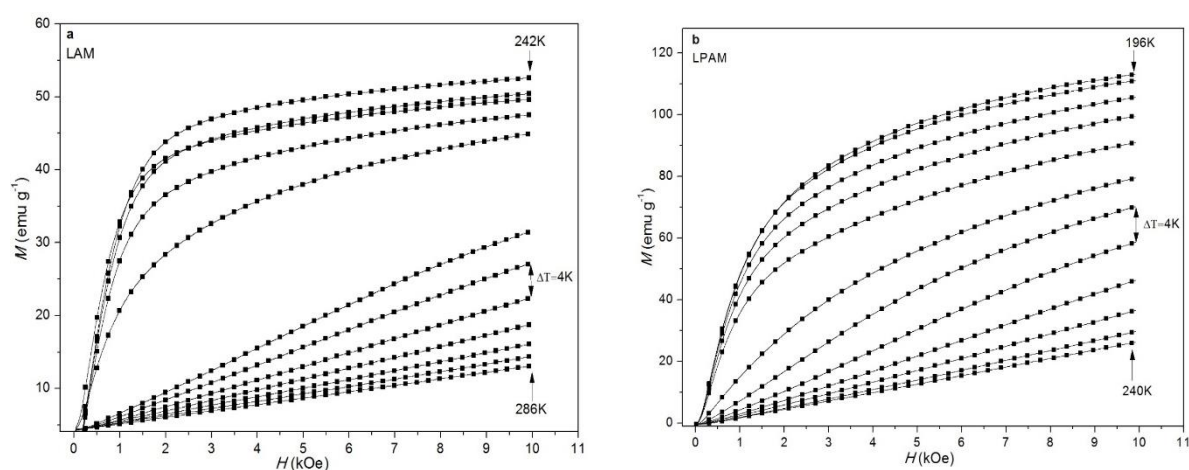


Fig. 1. a-b Magnetic field dependences of the magnetization at the temperatures from 242 K to 286 K and 196 K to 240 K ($\Delta T = 4$ K) for the La_{0.85}Ag_{0.15}MnO₃ and (La_{0.8}Pr_{0.2})_{0.85}Ag_{0.15}MnO₃ samples, respectively.

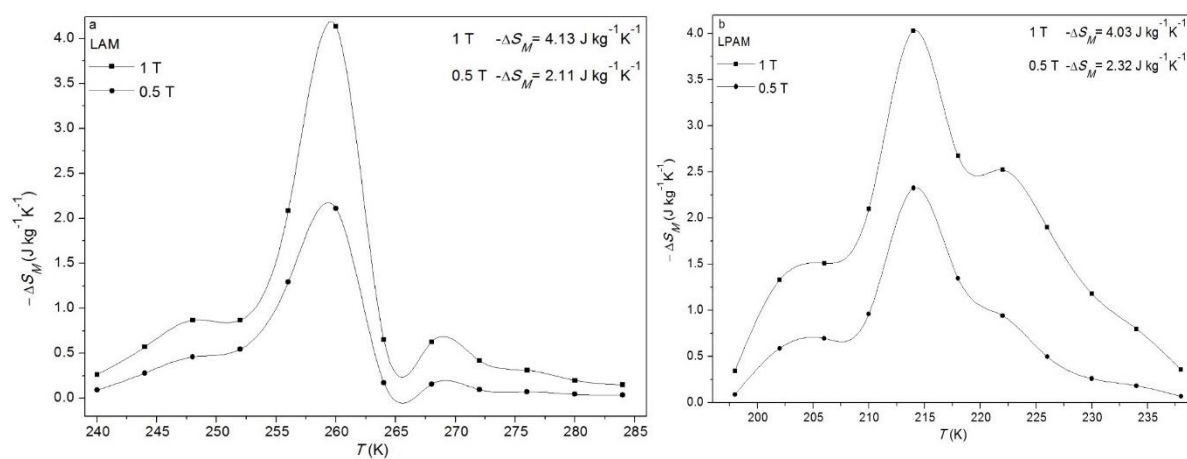


Fig.2.a-b The temperature dependence of ΔS_M for the $\text{La}_{0.85}\text{Ag}_{0.15}\text{MnO}_3$ and $(\text{La}_{0.8}\text{Pr}_{0.2})_{0.85}\text{Ag}_{0.15}\text{MnO}_3$ samples at 0.5 and 1 T magnetic fields.

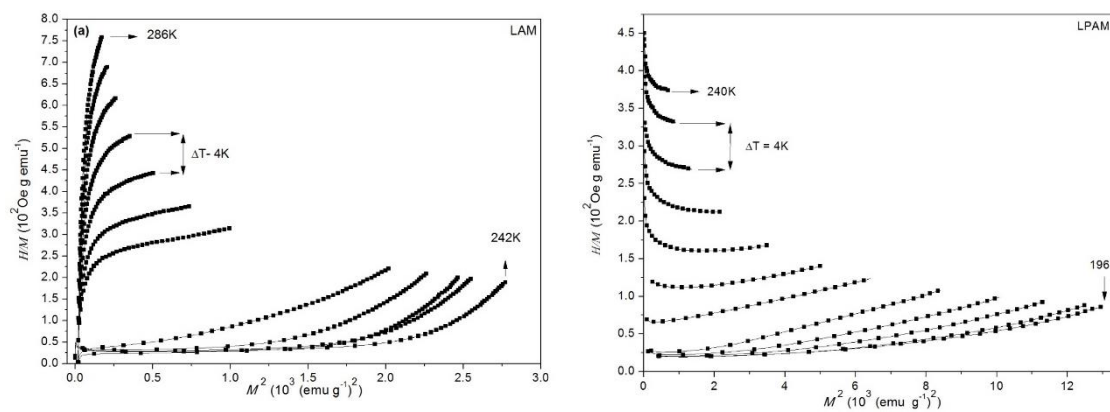


Fig. 3a-b. H/M vs. M^2 plots around T_C .